Prediction of Lung Cancer from Low-Resolution Nodules in CT-Scan Images by using Deep Features

Anand Gupta
Division of Computer Engineering
Netaji Subhas Institute of Technology
New Delhi, India
omaranand@nsitonline.in

Sagorika Das, Tarasha Khurana, Kamakshi Suri
Division of Computer Engineering
Netaji Subhas Institute of Technology
New Delhi, India
{sagorikad.co, tarashak.co, kamakshis.co}@nsit.net.in

***Abstract*—Prediction of lung cancer from CT-scan images is viewed as a challenging task in medical image analysis. It is because pulmonary nodules occupy less than 5% of a CT-scan image and vary highly in terms of their shape, texture, opacity and location, making it difficult to analyze by naked eye. To overcome this challenge, multiple approaches using digital processing of CT-scans are proposed. These existing approaches lack in addressing three main challenges in lung cancer prediction: *the problem of low resolution data, lack of generalized nodule features, and cancer prediction in terms of a malignancy score*. These challenges are addressed in the paper. In the proposed approach, CT-scan images are preprocessed and super-resolved to serve as input to a convolutional neural network for nodule region detection. Deep features engineered from different layers of this convolutional neural network are classified into two classes: benign and malignant. Additionally, these features are passed through a regressor to predict malignancy score. CT-scan images from a subset of the LIDC-IDRI dataset, called the LUNA16 dataset, are used for experimentation. An accuracy of 85.7% is achieved for the nodule classification task using the approach proposed in this paper, which is a substantial improvement over previous works in literature.**

***Index Terms*—lung cancer prediction, super-resolution, deep features, malignancy score, ct-scan images**

I. Introduction

Cancer is one of the most prominent diseases which contributes majorly to the world's mortality rate. Statistics show that, in the world there are 83 cancer deaths for every 100,000 females and 126 for every 100,000 men. Further, world's mortality rate also highlights that about 19% of deaths caused by cancer occur solely due to lung cancer, symbolizing it as one of the leading causes of cancer related deaths. It is characterized by the uncontrollable cell division in lung tissues. These irregularities in tissues are also known as pulmonary nodules. As shown in Fig. 1, pulmonary nodules are small, oval-shaped and vary from 5 to 30 millimeters in diameter. Although, nodules are detectable by low dose CT-scans yet precise characterization of this lesion growth is complicated for the naked eye due to its small size. A great amount of expertise is required by radiologists to correctly detect cancerous nodules. Hence, at earlier stages, these pulmonary nodules remain undetected. Accurately predicting the degree of malignancy at an initial stage has a great significance as it helps to improve the effectiveness of treatment and relieve patients from unnecessary stress. Thus, the problem of efficient detection and classification of cancerous pulmonary nodules is of great importance.

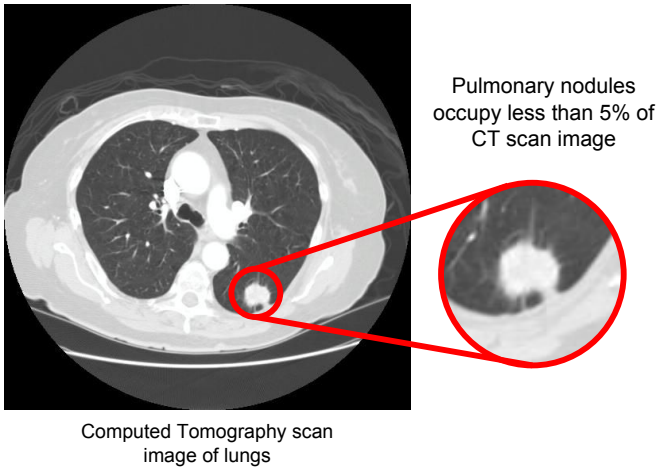

Fig. 1. Pulmonary nodule in a CT-scan image

For the above problem, recent systems proposed in this problem domain possess high sensitivity to cancer prediction but lack in reducing the number of false positives. In these works, the general approach for lung cancer prediction follows the given sequence:

1) **Nodule Detection** It is performed first as the pulmonary nodules occupy very less area on a lung CT-scan. As discussed by some approaches [6], [8], [9], it is important to localize these pulmonary nodules with respect to the lung before classifying them into benign (non-cancerous) and malignant (cancerous) tissues.
2) **Nodule Classification** It benefits from the previous step by extracting features for only the localized pulmonary nodules and then using a statistical classifier for their classification.

To have a better understanding of the previous approaches and the key challenges in this domain, existing research published in both the individual steps discussed above is surveyed and analyzed in Section I-A.

978-1-5386-5314-2/18/$31.00 ©2018 IEEE

A. Related Work

There are two categories of articles related to the research presented in this paper. These progressively discuss the task of detection of nodule regions in a CT-scan image, followed by their classification.

Nodule Detection As CT-scan images of lungs provide detailed view of blood vessels, soft tissues, muscle tissues and other organs like heart, stomach and pancreas, identification of boundaries of lung region from CT-scan is performed as a prior step to nodule detection as it reduces the search space for nodules. Several techniques such as k-means clustering by Gurcan *et al*. [1], thresholding approach by Zhao *et al*. [4], Hough transform by Orozco *et al*. [8] and bit plane slicing algorithm by Gomathi *et al*. [9] have been proposed for lung segmentation.

Next, nodules are detected in the segmented lung region in order to focus the attention area of the nodule classification system used in the succeeding stage. This can be done by using rule-based features and applying statistical classifiers on them as proposed by Gurcan *et al*. [1]. In other approach proposed by Kuppusamy *et al*. [2], nodules are detected using feature extraction followed by clustering. A template-matching technique proposed by Enquobahrie *et al*. [3] can also be employed to detect lung nodules. It is based on a genetic algorithm which determines the target position in the CT-scan image efficiently and selects an appropriate template image from several reference patterns for quick template matching. Artificial neural network ensemble approach as proposed by Zhou *et al*. [5] can also be put into action to identify lung cancer nodules in the images.

Nodule Classification Detected nodules are then classified as cancerous or non-cancerous. In the work of John *et al*. [10], multilevel thresholding based feature extraction is used for nodule classification. Lately, CAD systems have gained a lot of popularity for nodule classification and multiple models like [6], [8], [9] have been proposed for the same. In the work of Kumar *et al*. [6], a CAD system which uses deep features extracted from an autoencoder to classify nodules is proposed. Similarly in the work of Orozco *et al*. [8], a CAD system based on wavelet feature descriptor and support vector machine is proposed. Till now, CAD systems possess high sensitivity to cancer prediction but lack in reducing the number of false positives. With the advent of deep learning, the techniques such as deep belief networks are used as a replacement for nodule classification as proposed by Hua *et al*. [11].

All aforementioned approaches have been studied and their limitations have led to the formulation of a few key challenges. These are discussed in Section I-B.

B. Challenges

The drawbacks of the approaches mentioned above impose some challenges to develop a system that gives improved accuracy for prediction of lung cancer from CT-scan images. These are:

Low resolution data LUNA16 dataset [16] contains nodule regions of size as small as 20px. It proves to be a significant hindrance to the ability to train convolutional models from scratch because of low resolution features. Here the challenge is to propose an approach which works well even with low resolution data.

Lack of generalization Many rule-based approaches like [1], [3], depend upon traditional features in order to detect and classify nodules from CT-scan images. They tend to discard other unobservable features and therefore lack robustness. Hence, the challenge becomes extracting features from nodule regions such that these features are able to generalize well on the classification of unseen data *i.e.* generalization from training set to test set.

No information on degree of malignancy Another challenge is to provide information about the degree of malignancy. Most of the approaches like [4], [5] are limited to binary classification of nodules into benign and malignant types and do not say anything about "how" malignant a nodule is.

C. Contribution

The contributions of the paper keeping in mind the challenges discussed in Section I-B are as follows:

1) The approach proposed for predicting lung cancer works well with low resolution data. The technique of Single Image Super-Resolution [15] is employed to output high resolution images of the corresponding low resolution images by employing a deep convolutional neural network.
2) The proposed approach makes use of a convolution neural network to detect pulmonary nodules from CT-scan images. Deep features from different layers of this network are used for classification. The dependence on only observable features is thus removed and the use of deep-learned features makes the approach generalized and robust.
3) The approach is augmented with an additional stage where the deep-learned features extracted for different nodule regions are passed through a regressor and a malignancy score is predicted. This enables prediction of "how much" cancerous a nodule is rather than just the prediction of "if" the nodule is cancerous.

D. Organisation

The approach proposed in this paper is discussed in Section II. Dataset and training details of the convolutional neural network are given in Section III. Section IV provides a thorough analysis of the experimental results and the relative approach in this paper is concluded in Section V.

II. Proposed Approach

In this paper, a general lung cancer detection pipeline is enhanced by improving the resolution of input CT-scan regions and extracting their qualitative features from deep convolutional networks. Like any other lung cancer detection pipeline, the approach proposed in this paper is divided into three main stages as shown in Fig. 2. The stages are:

1) Data Preparation

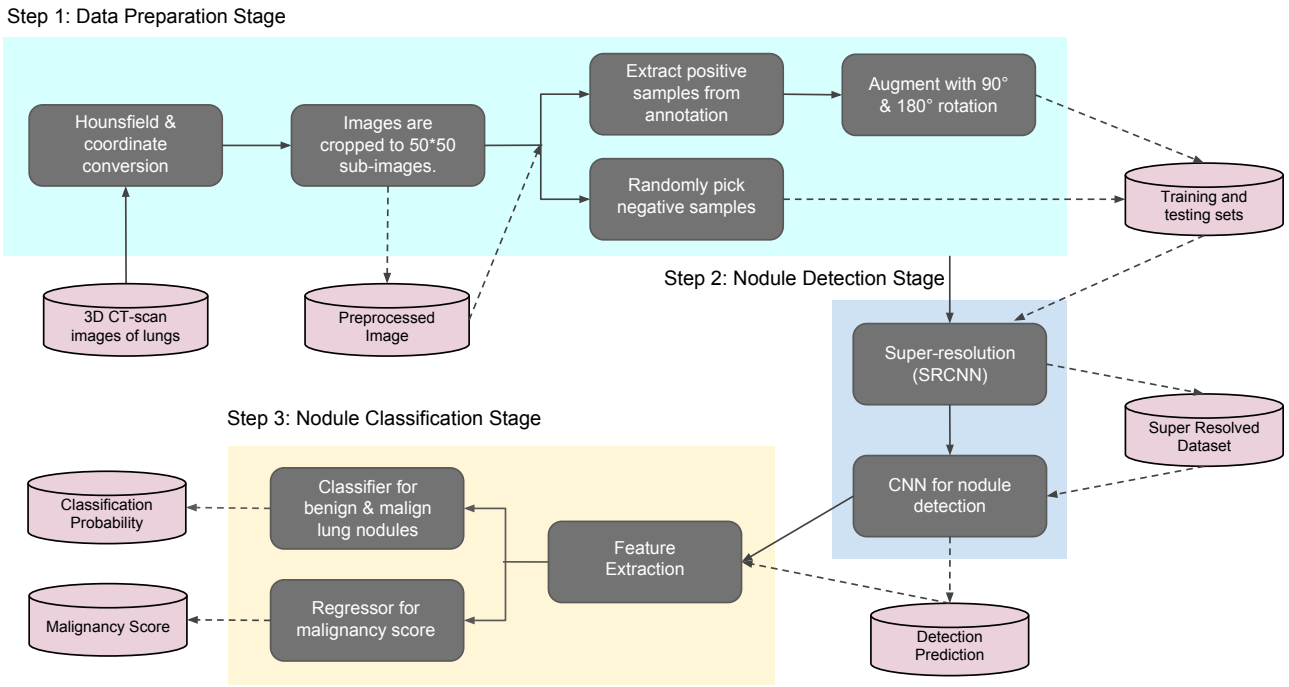

Fig. 2. Block Diagram of Proposed Approach

2) Nodule Detection
3) Nodule Classification

A. Data Preparation

The CT-scan images are first passed through the data preparation stage and the steps involved are depicted in Fig. 3. Initially Hounsfield Unit, which is a measure of radiodensity in CT-scan images, is converted to grayscale unit for image processing purposes. After this, annotations provided in the Cartesian coordinate system need to be converted to the Voxel coordinate system. This conversion is performed following which 50×50 pixel sub-images are cropped from around the nodule regions using the Voxel coordinates. Obtained 50×50 pixel grayscale images are then segregated into positive and negative samples. A total of 551,065 images are procured from the annotations, from which 1,351 are labeled as positive and rest as negative. To stabilize the imbalance in the ratio of positive and negative samples, 4k random negative samples are taken and the positive images are augmented by rotating by $90°$ and $180°$ to obtain a total of roughly 4k positive samples.

B. Nodule Detection

With the preprocessed CT-scan regions as input to this stage, nodule detection is carried out by using single image super-resolution (SR) on these images as the first step. As shown in Fig. 4, SR is performed in order to ensure that the following stage of Nodule Classification extracts good quality information from the low-resolution CT-scan regions in the form of more robust and qualitative features. This is done by deploying an end-to-end convolutional neural network called Super-Resolution Convolutional Neural Network (SRCNN) proposed by Dong *et al*. [15]. Single image super-resolution aims at recovering a high-resolution image from a single low-resolution image by learning a mapping function between these images. SRCNN learns this mapping by the means of three basic operations: patch extraction and representation, non-linear mapping and reconstruction. A forward pass through a pre-trained SRCNN gives as output, enhanced images of CT-scan regions and these are next sent to another convolutional neural network (CNN) for classifying CT-scan regions into nodule and non-nodule regions.

For this task of nodule region detection, pretrained ImageNet models of networks like AlexNet [19] and VGG16 [18] render themselves inefficient for use in this research. It is because the factors that explain the variation in ImageNet are very different from the factors affecting variation in a CT-scan image. Due to the high domain mismatch and inconsistency between the type, feature distribution and size of images used, transfer learning between these two domains is difficult. The architecture of the CNN used is shown in Fig. 5. Since, the input regions are only 50×50 pixel in size, the network is not very deep with only three convolutional layers and two fully connected layers. This architecture is arrived at after sufficient experimentation with different placements of the max pooling layers and different extent of dropout ratio. Increased amount of dropout reduces the required number of neurons in the network thus leading to underfitting. Less dropout makes the network prone to overfitting on training data. The right amount

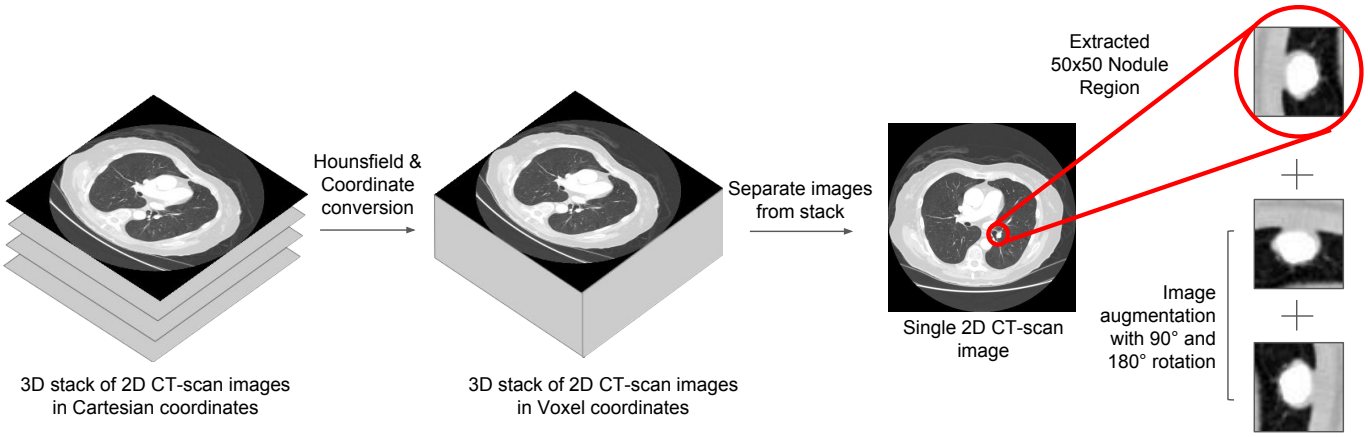

Fig. 3. Steps performed in Preprocessing

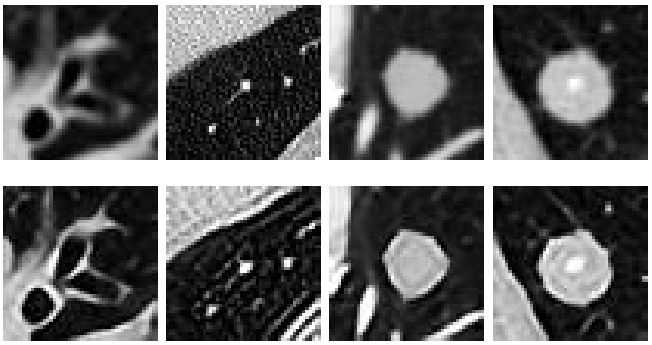

Fig. 4. **Single Image Super-Resolution using SRCNN [15]** First row shows original negative and positive samples from LUNA16 [14] dataset and second row shows the corresponding samples after passing samples through SRCNN [15].

of dropout along with sufficient data augmentation prevents the problem of overfitting.

The network performs binary classification on the given CT-scan regions into nodules or non-nodules. The predicted nodule regions are then sent to the next stage for classification into benign and malignant nodules.

C. Nodule Classification

Nodule regions are separated from the non-nodule ones in the Nodule Detection stage and the former are then classified into benign and malignant nodules. To execute this stage, every nodule region is forward passed through the nodule detection CNN and the layer outputs are utilised as a feature vector for classification. Different layers of the CNN model are investigated for their features. Fig. 7 (b) represents the deep features from a fully connected layer projected onto a 2D subspace. As shown in Fig. 6, extracted features are used as an input for a One-vs-All Support Vector Machine (SVM) to classify the nodules as cancerous or non-cancerous. Further, the extracted features are also passed through a Support Vector Regressor (SVR) to predict a score on a scale of 1-5 which stands for the degree of malignancy of nodule.

III. Experimental Setup

To implement the above approach, Python 3.5.2 with OpenCV, Keras and Scikit is used. The dataset used for the evaluation of the derived approach is described below.

For nodule detection and classification, images from the LUNA16 [16] dataset are used. LUNA16 dataset is a subset of the LIDC-IDRI [14] dataset which consists of 1,018 helical thoracic CT-scans along with associated XML files which contain two-phase image annotations performed by four thoracic radiologists. However, some scans are excluded as they have a section thickness greater than 2.5mm. A total of 888 CT-scans are included in LUNA16 dataset. The complete dataset is divided into 10 subsets and in each subset, CT-scan images are stored in MetaImage (mhd/raw) format. Each .mhd file is stored with a separate .raw binary file for the pixeldata.

In nodule detection stage, annotations for groundtruths are used from LUNA16 dataset. The nodule detection model is trained using the candidate nodule data which is stored in a Comma Separated Values (CSV) file. The file contains location of the candidate nodule regions and its corresponding class (0 for non-nodule and 1 for nodule).

The detected nodules are then sent to the classification stage, where the nodule is classified as benign or malignant. Malignancy information for the corresponding images is extracted from LIDC-IDRI annotations in which each nodule region is rated on a scale of 1-5 by four radiologists. The average malignancy rating is used for nodule classification and malignancy score prediction tasks. Nodules having a malignancy score greater than 3 are labelled as malignant and rest as benign. Traditional feature vectors used for experimentation are also designed using the LIDC-IDRI annotations.

The hyperparameters used in the training of the Nodule Detection CNN are detailed as follows. Categorical Cross Entropy loss is computed over the softmax activations of the last fully connected layer which has two output neurons. Adam optimizer is used for training with a learning rate of 0.001. This learning rate is kept constant throughout the training using a decay of zero. The network is trained for 50 epochs

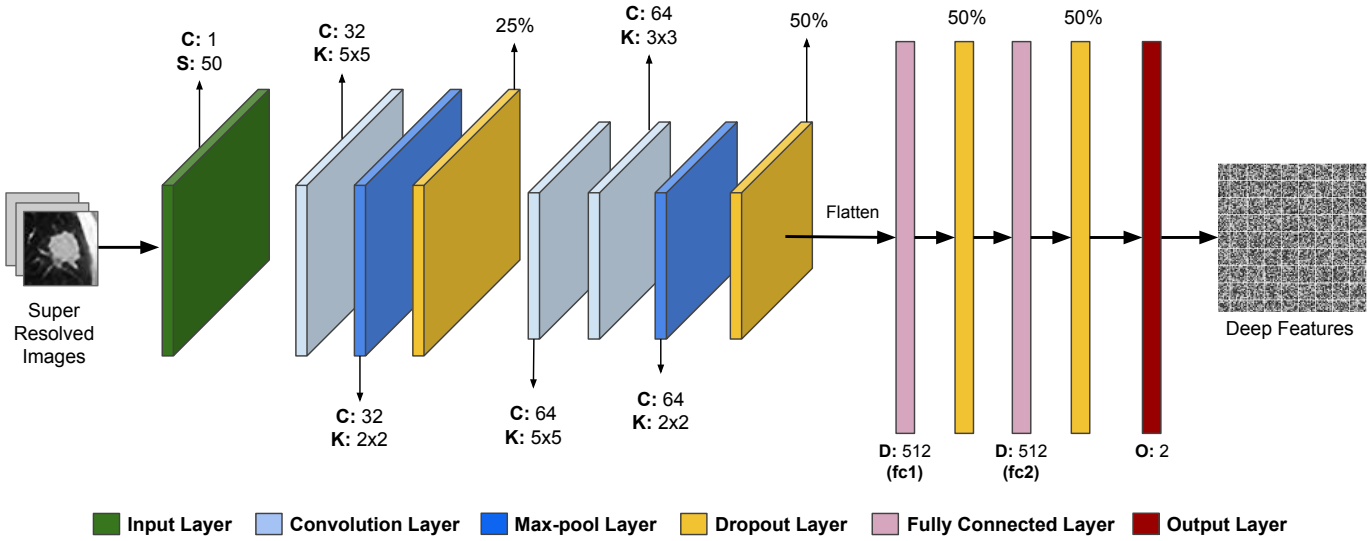

Fig. 5. **Architecture of CNN used for Nodule Detection** Image of size (S) is given as input to the CNN. Number of output channels (C) and the kernel size (K) are labeled for each subsequent layer. Extent of dropout is mentioned in % and the size of fully connected layers is given either in terms of their dimensionality (D) or the number of output neurons (O).

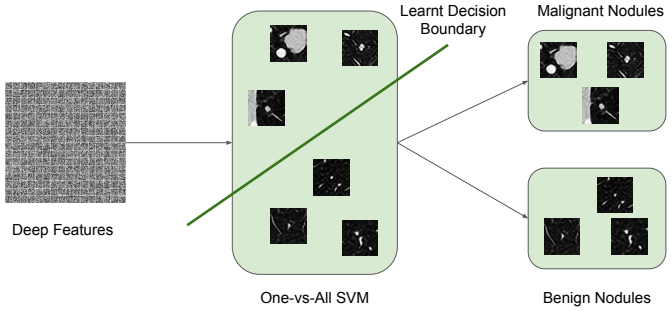

Fig. 6. Nodule Classification

till saturation. Batch size used for every iteration is 32. Ten-fold cross validation is performed using the 10 subsets given in the LUNA16 dataset. Accuracies reported in Section IV are an average of these ten cross validation accuracies.

IV. Result Discussion

In the past, lung cancer prediction algorithms have been successfully tested on the popular LUNA16 [16] dataset and LIDC-IDRI [14] dataset as they contain rich annotations of pulmonary nodules in CT-scan images. Hence, LUNA16 dataset along with corresponding annotations from LIDC-IDRI dataset is chosen to evaluate the proposed approach. Evaluation results of the approach are given in Table I and Table II.

In the proposed approach, the candidate nodule regions are super-resolved with the help of a neural network which learns an end-to-end mapping between the low-resolution and high-resolution images. From the results in Table I, it is evident that the technique of super-resolution improves the performance of the nodule detection network from 94.2% to 96.4%, showing an increase of 2.2%.

Further, deep features are extracted and used as an input to an SVM to recognize cancerous nodules. A comparison is drawn in Table II between traditional features like nodule size, shape, texture, opacity and location and deep features from different layers of CNN using both the original and super-resolved datasets. Results indicate that deep features notably enhance the classification accuracy. Features from the first fully connected (fc1) layer perform better than those extracted from the second fully connected (fc2) layer. It is found to be in accordance with the work of Vo *et al.* [17] who have postulated that the second last layer generalizes better on test data. With respect to traditional features, deep features from fc1 layer improve the lung cancer prediction accuracy from 84.1% to 84.9% using the original dataset and from 84.8% to 85.7% with super-resolved dataset resulting in an increase of 0.8% and 0.9% respectively. Therefore, the use of both super-resolution and deep features outputs a best accuracy of 85.7% for prediction of lung cancer from CT-scan images.

To highlight the generalization capability of deep features, the train and test set accuracies for nodule classification are recorded. It is done for two scenarios: (a) classification with super-resolution and traditional features and (b) classification with super-resolution and deep-learned features. The train and test accuracies in the first scenario are 91.3% and 84.8%, while for the second scenario these are 87.4% and 85.7% respectively. A high difference of 6.5% between the train and test accuracies in the first scenario clearly highlights that traditional features are overfit to the train set. A low difference of 1.7% in the case of deep-learned features shows that these features are able to generalize *i.e.* perform equally well on seen (train set) and unseen (test set) data. Decision

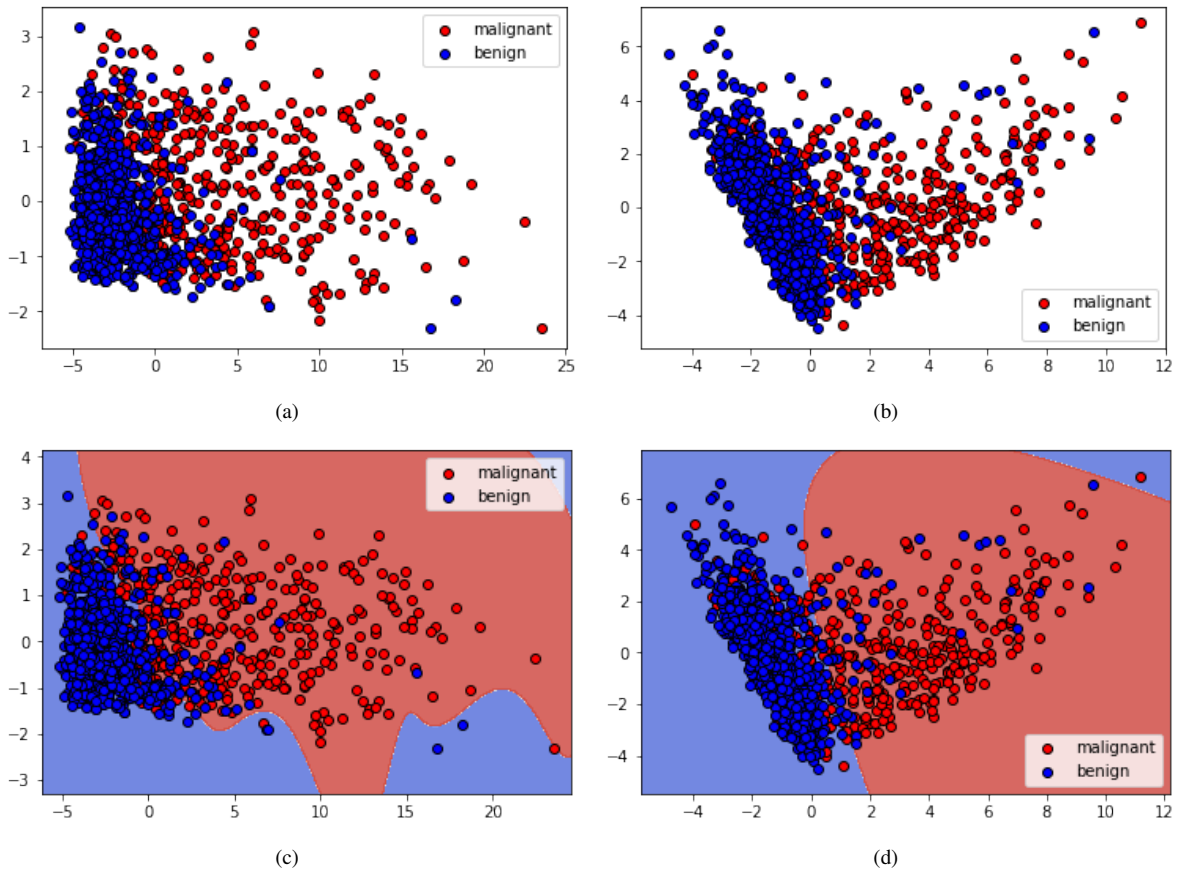

Fig. 7. **Feature Visualization** Traditional and deep features from the training set for benign and malignant nodule regions are illustrated by projecting them onto a 2D subspace using Principal Component Analysis [20] in (a) and (b) respectively. The decision boundaries learnt by the One-vs-All SVM for these two distributions are shown in (c) and (d) respectively.

TABLE I
PERFORMANCE ON NODULE DETECTION

	Absent	**Present**
Super-Resolution	94.2%	96.4%

TABLE II
PERFORMANCE ON NODULE CLASSIFICATION

	Original	**Super-Resolved**
Traditional Features	84.1%	84.8%
Deep Features (fc1)	84.9%	**85.7%**
Deep Features (fc2)	84.3%	85.1%

boundaries learnt by the SVM in these scenarios are also plotted in Fig. 7 (c) and Fig. 7 (d) respectively. The traditional feature vector and the 512-dimensional deep feature vector are projected onto a 2D subspace using Principal Component Analysis [20]. The learned decision boundaries for benign and malignant classes in the case of deep-learned features is less overfit to the 512-dimensional features in the training set than the traditional features. This again clearly depicts the generalisation capability of the deep-learned features.

The subsequent step of malignancy score prediction is evaluated using SVR over the extracted deep features. Performance is evaluated using the root-mean-square error (RMSE) metric which is a commonly used measure of the differences between values predicted by a model and the values observed. The RMSE metric is calculated to be 0.6431.

Table III shows a comparison between the approach proposed in this paper and the existing work for nodule classification. It can be clearly observed that the proposed approach outperforms the work of Kumar *et al*. [6], Silva *et al*. [12] and Song *et al*. [7] which test on the LIDC-IDRI dataset.

TABLE III
COMPARISON OF NODULE CLASSIFICATION PERFORMANCE WITH EXISTING WORK IN LITERATURE

Approach	**Classification Accuracy**
Kumar *et al*. [6]	75.01%
Silva *et al*. [12]	82.30%
Song (SAE) *et al*. [7]	82.59%
Song (CNN) *et al*. [7]	84.15%
Proposed Approach	**85.70%**

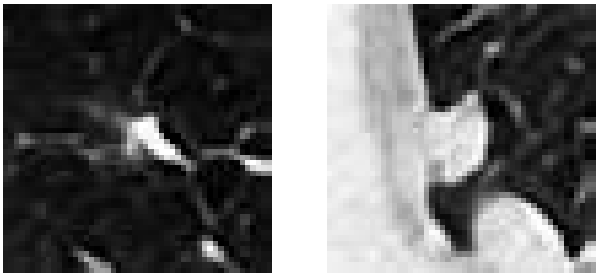

(a) (b)

Fig. 8. **Failure Cases** In (a), a nodule region is detected incorrectly as a non-nodule region possibly due to its small size during early stages of formation. In (b), a non-nodule region is falsely predicted to be a nodule region due to appearance similarity between nodules and other muscle tissues in the lung.

V. Conclusion

The paper provides a novel approach for predicting lung cancer from CT-scan images. The major challenges that are identified for this problem are overcome successfully by converting low-resolution nodule images into super-resolved images, extracting deep-learned features for making the approach more robust and predicting a malignancy score to give an accurate measure of a nodule's cancerous nature.

Using the above contributions, a thorough experimental analysis provides a nodule detection accuracy of 96.4% after the application of single image super-resolution. For nodule classification, features from the first fully connected layer of the nodule detection CNN yield an accuracy of 85.7% which is a substantial improvement over the previously proposed approaches like [6], [8], [12], [13]. It is also shown that deep features generalize better from training set to test set as compared to the traditional features used in previous approaches. Further, the proposed approach is able to achieve an RMSE value of 0.6431 for malignancy score prediction.

The results so obtained show that the proposed approach successfully detects nodules of different sizes present at various locations in a CT-scan. Some failure cases are shown in Fig. 8. As shown in Fig. 8 (a), nodules with extremely small size which grow with time into bigger and more apparent nodules are more prone to errors. This is because the proposed approach makes predictions using CT-scan at a single instance of time only whereas radiologists use CT-scans done at multiple instances of time to study a nodule for its malignancy. Temporal information related to a pulmonary nodule thus refines detection and prediction of lung cancer. Future work in this area can overcome the above failure cases by extending the proposed approach to a temporal model which itself learns to retain, forget or process temporal CT-scan data. For the same problem, a temporal CT-scan dataset can be built from multiple patients' CT-scans over a certain period of time.

References

[1] M. N. Gurcan, B. Sahiner, N. Petrick, H.-P. Chan, E. A. Kazerooni, P. N. Cascade, and L. Hadjiiski, "Lung nodule detection on thoracic computed tomography images: Preliminary evaluation of a computer-aided diagnosis system," Medical Physics, vol. 29, 2002, pp. 2552–2558.

[2] V. Kuppusamy, and R. C. Gopalakrishnan, "Feature Extraction Based Lung Nodule Detection in CT Images," International Journal of Applied Engineering Research, vol. 11, 2016, pp. 2697–2700.

[3] A. A. Enquobahrie, A. P. Reeves, D. F. Yankelevitz, and C. I. Henschke, "Automated detection of pulmonary nodules from whole lung helical CT scans: performance comparison for isolated and attached nodules," Medical Imaging 2004: Image Processing, vol. 5370, International Society for Optics and Photonics, 2004, pp. 791–801.

[4] B. Zhao, G. Gamsu, M. S. Ginsberg, L. Jiang, and L. H.Schwartz, "Automatic detection of small lung nodules on CT utilizing a local density maximum algorithm," Journal of Applied Clinical Medical Physic, vol. 4, 2003, pp. 248–260.

[5] Z.-H. Zhou, Y. Jiang, Y.-B. Yang, and S.-F. Chen, "Lung cancer cell identification based on artificial neural network ensembles," Artificial Intelligence in Medicine, vol. 24, 2002, pp. 25–36.

[6] D. Kumar, A. Wong, and D. A. Clausi, "Lung nodule classification using deep features in CT images," Computer and Robot Vision (CRV), 2015 12th Conference on, IEEE, 2015, pp. 133–138.

[7] Q. Song, L. Zhao, X. Luo, and X. Dou, "Using deep learning for classification of lung nodules on computed tomography images," Journal of healthcare engineering, 2017.

[8] H. M. Orozco, O. O. V. Villegas, V. G. C. Sánchez, H. d. J. O. Domínguez, and M. d. J. N. Alfaro, "Automated system for lung nodules classification based on wavelet feature descriptor and support vector machine," Biomedical engineering online, vol. 14, 2015, pp. 9.

[9] M. Gomathi, and P. Thangaraj, "A computer aided diagnosis system for lung cancer detection using support vector machine," American Journal of Applied Sciences, vol. 7, 2010, pp. 1532.

[10] J. John, and M. Mini, "Multilevel Thresholding Based Segmentation and Feature Extraction for Pulmonary Nodule Detection," Procedia Technology, vol. 24, 2016, pp. 957–963.

[11] K.-L. Hua, C.-H. Hsu, S. C. Hidayati, W.-H. Cheng, and Y.-J. Chen, "Computer-aided classification of lung nodules on computed tomography images via deep learning technique," OncoTargets and therapy, vol. 8, 2015.

[12] G. L. da Silva, A. C. Silva, A. C. de Paiva, and M. Gattass, "Classification of Malignancy of Lung Nodules in CT Images Using Convolutional Neural Network," OncoTargets and therapy.

[13] M. Hasna and J. Jose, "Lung Nodule Classification Using Multilevel Patch-based Context Analysis And Decision Tree Classifier," International Research Journal of Engineering and Technology (IRJET) e-ISSN, 2015, pp. 2395–0056.

[14] S. G. Armato, G. McLennan, L. Bidaut, M. F. McNitt-Gray, C. R. Meyer, A. P. Reeves, B. Zhao, D. R. Aberle, C. I. Henschke, E. A. Hoffman and others, "The lung image database consortium (LIDC) and image database resource initiative (IDRI): a completed reference database of lung nodules on CT scans," Medical physics, vol. 38, 2011, pp. 915–931.

[15] C. Dong, C. C. Loy, K. He and X. Tang, "Learning a deep convolutional network for image super-resolution," European Conference on Computer Vision, Springer, 2014, pp. 184–199.

[16] A. A. A. Setio, A. Traverso, T. De Bel, M. S. Berens, C. van den Bogaard, P. Cerello, H. Chen, Q. Dou, M. E. Fantacci, B. Geurts, et al, "Validation, comparison, and combination of algorithms for automatic detection of pulmonary nodules in computed tomography images: the LUNA16 challenge," Medical image analysis, vol. 42, 2017, pp. 1–13.

[17] N. Vo, and J. Hays, "Generalization in Metric Learning: Should the Embedding Layer be the Embedding Layer?," arXiv preprint arXiv:1803.03310, 2018.

[18] K. Simonyan and A. Zisserman, "Very deep convolutional networks for large-scale image recognition," arXiv preprint arXiv:1409.1556, 2014.

[19] A. Krizhevsky, I. Sutskever, and G. E. Hinton, "Imagenet classification with deep convolutional neural networks," Advances in neural information processing systems, 2012, pp. 1097–1105.

[20] K. Pearson, "LIII. On lines and planes of closest fit to systems of points in space," The London, Edinburgh, and Dublin Philosophical Magazine and Journal of Science, vol. 2, 1901, pp. 559–572.